Glycoconj J (2014) 31:71–87
DOI 10.1007/s10719-013-9504-8

Effect of distal sugars and interglycosidic linkage on the *N*-glycoprotein linkage region conformation: synthesis and X-Ray crystallographic investigation of β-1-*N*-alkanamide derivatives of cellobiose and maltose as disaccharide analogs of the conserved chitobiosylasparagine linkage

Manoharan Mathiselvam · Venkatachalam Ramkumar · Duraikkannu Loganathan · Serge Pérez

Received: 25 August 2013 / Revised: 7 October 2013 / Accepted: 7 October 2013 / Published online: 23 October 2013

Abstract The linkage region constituents, 2-deoxy-2-acetamido-β-D-glucopyranose (GlcNAc) and L-asparagine (Asn) are conserved in the *N*-glycoproteins of all eukaryotes. Elucidation of the structure and conformation of the linkage region of glycoproteins is important to understand the presentation and dynamics of the carbohydrate chain at the protein/cell surface. Earlier crystallographic studies using monosaccharide models and analogs of *N*-glycoprotein linkage region have shown that the *N*-glycosidic torsion, ϕ_N, is more influenced by the structural variation in the sugar part than that of the aglycon moiety. To access the influence of distal sugar as well as interglycosidic linkage (α or β) on the *N*-glycosidic torsion angles, cellobiosyl and maltosyl alkanamides have been synthesized and structural features of seven of these analogs have been characterized by X-ray crystallography. Comparative analysis of the seven disaccharide analogs with the reported monosaccharide analogs showed that the ϕ_N value of cellobiosyl analogs deviate ~9° with respect to GlcβNHAc. In the case of maltosyl analogs, deviation is more than 18°. These deviations indicate that the *N*-glycosidic torsion is influenced by addition of distal sugar as well as with respect to inter glycosidic linkage (α or β); it is less influenced by changes occurring at the aglycon. The χ_2 value of alkanamide derived from glucose, cellobiose and maltose exhibit a large range of variations (from 1.6° to −109.9°). This large span of χ_2 value suggests the greater degree of rotational freedom around C1′-C2′ bond which is restricted in GlcNAc alkanamides. The present finding explicitly proved the importance of molecular architecture in the *N*-glycoproteins linkage region to maintain the linearity, planarity and rigidity. These factors are necessary for *N*-glycan to serve role in inter- as well as intramolecular carbohydrate-protein interactions.

Keywords Glycoprotein · *N*-Glycoprotein linkage region analogs · *N*-Acetylglucosamine · Trifurcated hydrogen bond · X-ray · Crystal structure

Duraikkannu Loganathan was deceased on February 9, 2013.

Electronic supplementary material The online version of this article (doi:10.1007/s10719-013-9504-8) contains supplementary material, which is available to authorized users.

M. Mathiselvam (✉) · V. Ramkumar · D. Loganathan
Department of Chemistry, Indian Institute of Technology Madras, Chennai 600036, India
e-mail: mathi24@gmail.com

S. Pérez (✉)
Centre de Recherches sur les Macromolécules Végétales Grenoble cedex, CNRS affiliated with Universite Grenoble, BP 53X, 38041 Grenoble cedex, France
e-mail: serge.perez@cermav.cnrs.fr

S. Pérez
e-mail: spsergeperez@gmail.com

Abbreviations

GlcNAcβNHAc	*N*-(2-deoxy-2-acetamido-β-D-glucopyranosyl)acetamide
NMR	Nuclear Magnetic Resonance
ESI-MS	Electrospray Ionization Mass Spectrometry
ORTEP	Oak Ridge Thermal Ellipsoid Plot

Introduction

The glycan part of glycoproteins is involved in wide range of biological processes such as signal transduction, protein folding, targeting, stability, cell-cell and cell-matrix interactions [1–4]. It is essential to understand the structure-function correlations of the protein-linked glycans. The linkage region constituents, 2-deoxy-2-acetamido-β-D-glucopyranose (GlcNAc) and L-asparagine (Asn), are conserved in the *N*-glycoproteins of all eukaryotes [5]. Elucidation of the structure and conformation of the *N*-glycoprotein linkage region (GlcNAcβAsn) is of importance to understand the presentation and dynamics of the carbohydrate chain at the protein surface. Earlier studies by 2D-NMR using model glycopeptides showed the influence of glycosylation and importance of molecular architecture in *N*-glycoprotein linkage region [6–9]. Inherent flexibility and microheterogeneity of carbohydrates attached to proteins complicates crystallographic analysis of glycoproteins. Due to the above reasons, their X-ray structural studies are limited. Use of model compounds and analogs is a valuable approach to understand the effect of structural variations on the linkage region conformation.

As part of a research program aimed at understanding the structural significance of the constituents of the *N*-glycoprotein linkage region, we have earlier reported the results of a systematic investigation among several β-*N*-glycopyranosylamido derivatives [10–22]. In those studies, we have systematically analyzed the linkage region conformations as defined by torsion angles ϕ_N (O5–C1–N1–C1′), ψ_N (C1–N1–C1′–C2′) and χ_2 (N1–C1′–C2′–C3′) (Fig. 1). The variation in these torsion angles affects the planarity and rigidity of linkage region. These studies illustrated the effect of structural variation in the linkage region sugar and its aglycon moiety on the conformation when compared to the crystal structures of GlcNAcβAsn [23, 24]. For example, the results of the crystallographic analysis of several *N*-(β-glycopyranosyl)alkanamides derived from monosaccharides revealed significant variations in ϕ_N up to 31° (XylβNHAc) from the value observed for the model compound GlcNAcβNHAc [13]. The conformation of the torsion angle ϕ_N is mainly influenced by neighboring group such as C2-acetamido [16, 17], by regular (O–H···O) hydrogen bonds; weak C–H···O contacts play a role as well. These studies suggest that φ_N is influenced to a larger extent by the structural variation of the sugar part than that of the aglycon moiety. Ab initio quantum chemical calculations and X-ray crystallographic studies on propionamido and chloroacetamido derivatives showed the critical role of the C2-acetamido group of GlcNAc in controlling χ_2 at the linkage region of *N*-glycoproteins and conserving the extended side chain conformation [15]. A comprehensive analysis of non covalent interactions present in the crystal structures of 12 *N*-glycoprotein models and analogs showed a unique antiparallel double pillared bifurcated hydrogen bonding pattern in the model compound GlcNAcβNHAc as well as in GlcNAcβAsn [18]. This observation was also confirmed by low-temperature neutron crystal structure analysis of three monosaccharide glycosyl alkanamide derivatives which provides high resolution geometrical parameters of the *N*-glycoprotein linkage region [19].

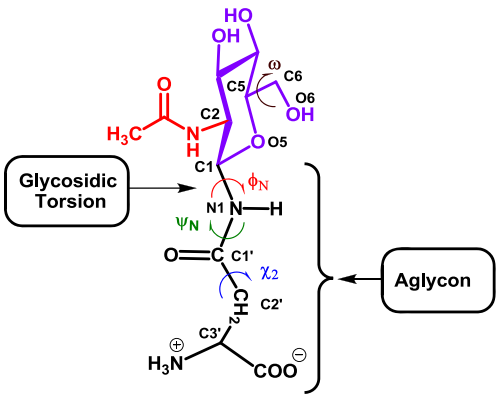

Fig. 1 Schematic representation of the linkage region (GlcNAcβAsn) of the *N*-glycoproteins with the depiction of torsion angles, ω=O5–C5–C6–O6, ϕ_N=O5–C1–N1–C1′, ψ_N=C1–N1–C1′–C2′ and χ_2=N1–C1′–C2′–C3′

The present work was undertaken to understand the effect of distal sugar as well as interglycosidic linkage (α or β) on the *N*-glycosidic torsion. To accomplish these objectives, several disaccharide (cellobiosyl and maltosyl)alkanamides (Fig. 2) have been synthesized as analogs of the *N*-glycoprotein linkage region. Comparative analysis of crystal structures of alkanamido derivatives of cellobiose and maltose, along with those reported for glucose, highlighted the influence of the distal sugar on linkage region conformation.

Results and discussion

Synthesis of *N*-{(4-*O*-(D-glucopyranosyl) -β-D-glucopyranosyl}alkanamides

The preparation of glycosyl alkanamides (**4**–**11**) was started with cellobiose or maltose. The disaccharides were converted into their respective glycosyl amine by treating with ammonium bicarbonate [25]. The cellobiosyl and maltosyl amines were reacted with anhydride to give the cellobiosyl (**4**–**7**, 23–30 %) and maltosyl alkanamides (**8**–**11**, 36–53 %), respectively (Scheme 1).

X-Ray crystallographic investigation

Crystal structure description

With the exception of the propionamide derived from cellobiose (**5**), crystals suitable for X-ray analysis were obtained by

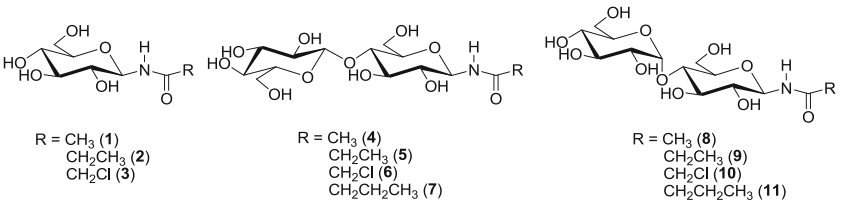

Fig. 2 Mono (**1**–**3**) and disaccharide (**4**–**11**) analogs of *N*-glycoprotein linkage region

crystallization from aqueous methanol. Crystal structures were solved in the space group P_1 for **4**, $P2_1$ for **6 & 7** and in $P2_12_12_1$ for all the four maltosyl alkanamide derivatives (**8**–**11**). All the disaccharide alkanamides crystallize as dihydrates. In addition to two water molecules, cellobiosyl butanamide (**7**) has one methanol molecule in its crystal lattice. ORTEP representations of the crystal structures of **4**, **6–11** along with the numbering of the atoms are shown in Fig. 3. The pyranose rings exists in the usual $^4C_1$ conformation in all the structures. The Cremer-Pople puckering parameters for the seven compounds are given in Table 1. Displacement (Å) of C1 and C4 atoms from the C2, C3, C5, and O-5 least-square plane of compounds **4** & **6**–**11** are given in Table 2. A list of selected bond lengths and bond angles is given in Table 3. All the C–C bond lengths are close to 1.54 Å, which is observed in most sugar derivatives [26]. The endocyclic C–O bond distances, namely, C1A–O5A, C5A–O5A of proximal sugar and C1B–O5B, C5B–O5B of distal sugar of all the analogs follow the normal trend of the latter in each case being longer than the former. This shortening is attributed to the stabilizing effect of the delocalization of the nitrogen lone pair of electrons into the anti-bonding orbital of the C1A–O5A bond. The above mentioned delocalization also shortens the C1A–N1 bond distance compared to alkyl chain C–N distance of 1.50 and 1.55 Å in the two independent molecules present in the asymmetric unit of *N*-methylchloroacetamide [27]. The C1A–N1 bond distances of 1.41–1.44 Å of compounds (**4** & **6**–**11**) are in good agreement with the value of 1.44 Å reported for GlcNAcβAsn [24]. The C2′–Cl bond lengths of **6** and **10** are found to be 1.750(4) and 1.698(6) Å, respectively. Comparison of these values with the value of 1.752(5) Å noted for GlcβNHCOCH$_2$Cl (**3**) [12] shows the largest difference between those of **3** and **10**. The exocyclic C6A–O6A and C6B–O6B bond distances are in the range of 1.40–1.43 Å which is in good agreement with the normal C–O bond distance.

All the angles involving carbons are close to the tetrahedral value of 109.5° while those involving nitrogen are in the trigonal range. These bond angles of all the analogs (**4** & **6**–**11**) are comparable to that of GlcNAcβAsn. The slight deviation noted in exocyclic bond angles namely C4A–C5A–C6A, C4B–C5B–C6B, O5A–C5A–C6A and O5B–C5B–C6B, has also been observed for GlcNAcβAsn. It is attributed to the effect of the lone pair of electrons on the oxygen causing the bend on the O5A–C5A–C6A and O5B–C5B–C6B bond angles. The *N*-glycosidic valence angle, O5A–C1A–N1, is smaller than that of C2A–C1A–N1 for **4** & **6**–**11**; the same trend was consistently seen in all the models and analogs examined. The valence angle involving chlorine atom, C1′–C2′–Cl, of **6** and **10** are 116.4° and 111.2° respectively, the former one is 5.5° larger than the value (110.9°) reported for the GlcβNHCOCH$_2$Cl (**3**).

Molecular conformations

The conformations of the cellobiosyl (**4**, **6 & 7**) and maltosyl (**8**–**11**) alkanamides are defined by the torsion angles ω_B, ω'_B, ϕ_0, ψ_0, ω_A, ω'_A, ϕ_N, ψ_N and χ_2 (Fig. 4). The molecular conformations are compared with those of corresponding monosaccharide alkanamides GlcβNHAc (**1**) [10], GlcβNHPr (**2**) [13] and GlcβNHCOCH$_2$Cl (**3**) [12] to understand the influence of additional sugar as well as interglycosidic conformation on the linkage region. Selected torsion angles of the glucosyl (**1**–**3**), cellobiosyl (**4**, **6 & 7**) and maltosyl (**8**–**11**) alkanamides are presented in Table 4.

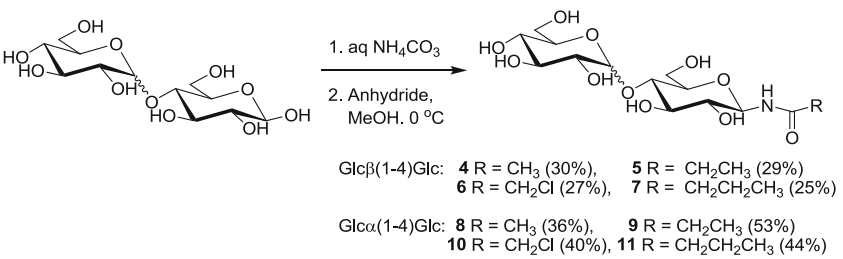

Scheme 1 Preparation of *N*-{(4-*O*-(D-glucopyranosyl)-β-D-glucopyranosyl}alkanamides (**4**–**11**)

Cellobiosyl alkanamides (**4**, **6 & 7**)

The values of *N*-glycosidic torsion ϕ_N observed for cellobiosyl alkanamides (**4**, **6 & 7**) are −101.8°, −101.9° and −103.5°, respectively (Table 4). These torsion angles are deviating to a maximum of ~9° and ~12° when compared to those of the analog GlcβNHAc (**1**) (−93.7°) [10] and model GlcNAcβNHAc (−89.8°) [11], respectively. The deviation noted among the cellobiosyl alkanamides (**4**, **6 & 7**) is negligible. A similar trend was noted among the glucosyl alkanamides (**1**–**3**) [13] (Fig. 5). The ψ_N values of cellobiosyl alkanamides **4**, **6 & 7** are around 174° which was noted for the model compound GlcNAcβNHAc [11]. Based on the observed values of ϕ_N and ψ_N, one can conclude that the conformation of the *N*-glycosidic linkage in **4**, **6 & 7** is *Z-anti*. The χ_2 values of cellobiosyl alkanamides **6** and **7** are 1.6° and −100.2°,

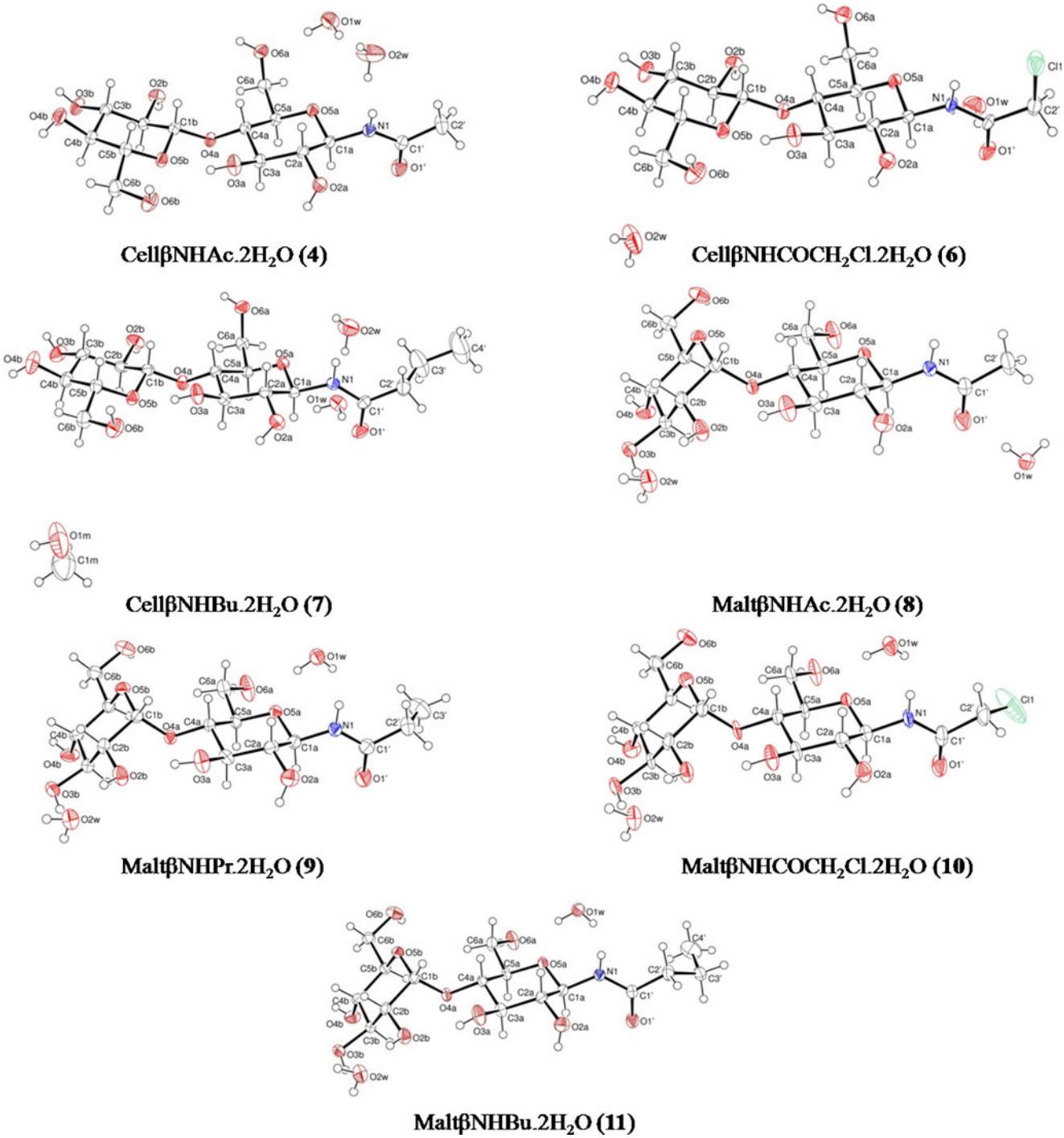

Fig. 3 ORTEP representation (40 % probability) of cellobiosyl (**4**, **6**–**7**) and maltosyl (**8**–**11**) alkanamides

respectively whereas those reported earlier for glucosyl alkanamides are 114.7° (**2**) and 131.3° (**3**) (Table 4, Fig. 6). The deviation of χ_2 value among cellobiosyl alkanamides (**6 & 7**) is significantly higher when compared to those of glucosyl alkanamides (**2 & 3**). Apart from the intrinsic torsional energy, the *N*-glycosidic torsion angles are mainly influenced by C2-NHAc group and molecular packing. In absence of C2-NHAc group in cellobiosyl alkanamides (**4**, **6 & 7**), molecular packing could be the influencing factor for *N*-glycosidic torsion values. In the cellobiosyl alkanamides (**4**, **6 & 7**), the interglycosidic torsion angle ϕ_0 value (C4A–O4A–C1B–O5B) is around −90° and ψ_0 (C1B–O4A–C4A–C5A) value is in between −145.9° and −153.0° (Table 4). These angles compare well with those reported for cellobiose related structures [28, 29]. The ω & ω' values (Table 4) indicate that the exocyclic hydroxymethyl group in cellobiosyl alkanamides (**4**, **6 & 7**) adopts *gg* conformation in the proximal ring and *gt* conformation in the distal ring [30].

Maltosyl alkanamides (**8–11**)

The ϕ_N values of maltosyl alkanamides **8**–**10** are −111.5°, −109.7° and −112.2°, respectively. These values deviate by ~18º when compared to the value of −93.7º reported for GlcβNHAc (**1**). In the case of maltosyl butanamide (**11**) however, the ϕ_N value is −123.4° showing a maximum deviation of 29.6° (Table 4, Fig. 5). The ψ_N values of maltosyl alkanamides (**8**–**11**) are in the range of −170.3° to 179.5°. Thus, the aglycon moieties of **8**–**11** adopt *Z-anti* conformation. The χ_2 values of maltosyl alkanamides **9**–**11** are −109.9°, −133.4° and −143.1°, respectively (Table 4, Fig. 6). Similar to cellobiosyl alkanamides (**4**, **6 & 7**), maltosyl alkanamides (**8**–**11**) also showed wide deviation in the *N*-glycosidic torsion angles which could be due to the molecular packing. The interglycosidic torsion angle ϕ_0 values of **8**–**11** are around 102° and the ψ_0 values turn out to be in the range of −132.6º to −135.5º (Table 4). The ω & ω' values (Table 4) indicate that all of the hydroxymethyl group of maltosyl alkanamides **8**–**11** adopts *gt* conformation in both proximal & distal rings.

Molecular packing

*Cellobiosyl alkanamides (**4**, **6 & 7**)*

Molecular packing of all the cellobiosyl alkanamides **4**, **6 & 7** is stabilized by an extensive network of regular hydrogen bonds as well as C−H···O and hydrophobic interactions (Figs. 7 and 8, Tables 5 and 6). All the cellobiosyl analogs **4**, **6 & 7** display identical packing features excepting the insertion of a methanol molecule into the crystal structure of the butanamide analog (**7**). There are three finite chains and one infinite chain of hydrogen bonds present in cellobiosyl alkanamides (Table 7). The first finite chain of hydrogen bonding connects N1-H1N to O1′. The second finite chain starts from O4B, passes through two water molecules and ends at O1′. Thus, O1′ is a bifurcated acceptor for both the finite chains. The third relatively long finite chain starts with O4B, runs through O2W, O1W, O6A, O2A, O2B, O3A and ends at O5B. In the case of cellobiosyl butanamide (**7**) one methanol molecule is inserted in this chain between O4B and O2W. Intramolecular hydrogen bond between O3A as a donor and O5B as an acceptor is the barrier for rotation about the interglycosidic bond which is also observed in other cellobiosyl derivatives [28]. Unlike methyl cellobioside, the hydrogen bond between O3A and O6B is not seen due to longer O3A-H···O6B distances. This hydrogen bond is known to facilitate the occurrence of *gt* conformation around β(1–4)linkages [29]. The zig-zag type of infinite chain of hydrogen bonding involves ···O6B–H6OB···O3B–H3OB··· propagating along the crystallographic a-axis (Fig. 8). One water molecule (O1W) is tetra co-ordinated and the other (O2W) is tri co-ordinated. The tri co-ordinated water molecule O2W donates both of its hydrogen atoms to the tetra co-ordinated water molecule O1W, thereby forming a water channel along the crystallographic a-axis (Fig. 9). Although the regular hydrogen

Table 1 Cremer-Pople puckering parameters of compounds **4** & **6**–**11**

Compound code and no.	Ring A			Ring B		
	Q	*θ*	*ϕ*	*Q*	*θ*	*ϕ*
CellβNHAc.2H_2O (**4**)	0.5619(16) Å	4.95(15)°	20.8(19)°	0.5808(16) Å	12.75(16)°	70.6(7)°
CellβNHCOCH_2Cl.2H_2O (**6**)	0.553(4)Å	6.2(4)°	26(4)°	0.592(4)Å	11.9(4)°	73.1(18)°
CellβNHBu.2H_2O.MeOH (**7**)	0.5617(16)Å	6.55(16)°	14.5(15)°	0.5723(18)Å	8.22(19)°	50.7(13)°
MaltβNHAc.2H_2O (**8**)	0.5835(17)Å	0.38(16)°	356(15)°	0.5374(17)Å	3.14(18)°	64(3)°
MaltβNHPr.2H_2O (**9**)	0.5762(16)Å	1.31(16)°	99(7)°	0.5277(15)Å	5.20(16)°	42.6(18)°
MaltβNHCOCH_2Cl.2H_2O (**10**)	0.583(6)Å	0.0(6)°	82(24)°	0.512(6)Å	3.6(7)°	48(9)°
MaltβNHBu.2H_2O (**11**)	0.575(4)Å	0.8(4)°	289(81)°	0.532(4)Å	3.6(4)°	60(7)°

Table 2 Displacement (Å) of C-1 and C-4 atoms from the C-2, C-3, C-5, and O-5 least-square plane of compounds **4** & **6**–**11**

Parameter	CellβNHAc. $2H_2O$ (**4**)	CellβNHCO $CH_2Cl.2H_2O$ (**6**)	CellβNHBu. $2H_2O$.MeOH (**7**)	MaltβNHAc. $2H_2O$ (**8**)	MaltβNHPr. $2H_2O$ (**9**)	MaltβNHCO $CH_2Cl.2H_2O$ (**10**)	MaltβNHBu. $2H_2O$ (**11**)
Ring A							
C2A	−0.0238 (0.0008)	−0.0241 (0.0017)	−0.0319 (0.0008)	−0.0103 (0.0008)	−0.0086 (0.0019)	−0.0039 (0.0029)	−0.0026 (0.0007)
C3A	0.0227 (0.0007)	0.0230 (0.0016)	0.0304 (0.0007)	0.0100 (0.0008)	0.0083 (0.0018)	0.0038 (0.0028)	0.0025 (0.0007)
C5A	−0.0244 (0.0008)	−0.0243 (0.0017)	−0.0326 (0.0008)	−0.0106 (0.0008)	−0.0088 (0.0019)	−0.0040 (0.0029)	−0.0026 (0.0007)
O5A	0.0255 (0.0008)	0.0254 (0.0018)	0.0341 (0.0008)	0.0109 (0.0008)	0.0091 (0.0020)	0.0041 (0.0030)	0.0027 (0.0008)
C1A	−0.6764 (0.0021)	−0.6752 (0.0047)	−0.6803 (0.0021)	−0.6781 (0.0021)	−0.6644 (0.0052)	−0.6808 (0.0078)	−0.6772 (0.0020)
C4A	0.6322 (0.0022)	0.6119 (0.0050)	0.6287 (0.0024)	0.6849 (0.0023)	0.6795 (0.0055)	0.6736 (0.0084)	0.6690 (0.0022)
Ring B							
C2B	−0.0053 (0.0007)	−0.0076 (0.0017)	0.0141 (0.0008)	−0.0048 (0.0007)	−0.0054 (0.0018)	−0.0093 (0.0026)	−0.0125 (0.0007)
C3B	0.0049 (0.0007)	0.0072 (0.0016)	−0.0133 (0.0008)	0.0046 (0.0007)	0.0052 (0.0017)	0.0089 (0.0025)	0.0119 (0.0006)
C5B	−0.0052 (0.0007)	−0.0076 (0.0017)	0.0142 (0.0008)	−0.0049 (0.0007)	−0.0054 (0.0018)	−0.0093 (0.0026)	−0.0124 (0.0007)
O5B	0.0056 (0.0008)	0.0080 (0.0018)	−0.0150 (0.0009)	0.0051 (0.0008)	0.0057 (0.0019)	0.0097 (0.0027)	0.0130 (0.0007)
C1B	0.7442 (0.0020)	0.7535 (0.0048)	0.7156 (0.0022)	−0.6484 (0.0019)	−0.6460 (0.0046)	−0.6218 (0.0069)	−0.6491 (0.0018)
C4B	−0.5777 (0.0023)	−0.5977 (0.0056)	−0.6144 (0.0026)	0.6196 (0.0022)	0.6069 (0.0056)	0.5812 (0.0082)	0.5919 (0.0021)

bondings (O–H···O and N–H···O) are identical among **4**, **6** & **7**, their C–H···O interactions are different (Tables 6). The acetamide **4** and chloroacetamide **6** display four common C–H···O interactions (C3A–H3A···O2B, C6A–H6A2···O2A, C2B–H2B···O4B, C6B–H6B1···O2W) which render O2W as tetra co-ordinated and O2A & O2B as bifurcated acceptors. The chloroacetamide **6** shows an additional C–H···O interaction (C2A–H2A···O1′) that makes O1′ as a trifurcated acceptor. On the other hand, the cellobiosyl butanamide **7** displays only two C–H···O interactions (C5A–H5A···O6A and C6A–H6A2···O2A) which result in O6A & O2A serving as bifurcated acceptors. Furthermore, all the cellobiosyl alkanamides show one hydrophobic interaction C2B–H2B···H3B–C3B (2.20 Å) in the distal residue.

Table 3 Selected bond lengths (Á) and bond angles (°) of disaccharide alkanamides (**4**, **6**–**11**)

Parameter	CellβNHAc. $2H_2O$ (**4**)	CellβNHCO $CH_2Cl.2H_2O$ (**6**)	CellβNHBu. $2H_2O$.MeOH (**7**)	MaltβNHAc. $2H_2O$ (**8**)	MaltβNHPr. $2H_2O$ (**9**)	MaltβNHCO $CH_2Cl.2H_2O$ (**10**)	MaltβNHBu. $2H_2O$ (**11**)
C1A-O5A	1.419(2)	1.428(4)	1.425(2)	1.427(2)	1.424(4)	1.406(6)	1.427(2)
C5A-O5A	1.430(2)	1.438(5)	1.421(2)	1.431(2)	1.432(4)	1.421(6)	1.435 (2)
C6A-O6A	1.426(2)	1.429(5)	1.417(2)	1.420(2)	1.419(5)	1.400(6)	1.419(2)
C1A-N1	1.433(2)	1.435(5)	1.431(2)	1.429(2)	1.418(5)	1.413(7)	1.430(2)
C1′-N1	1.338(2)	1.340(5)	1.340(2)	1.334(2)	1.328(5)	1.315(8)	1.342(2)
C1′-O1′	1.226(2)	1.227(4)	1.237(2)	1.221(3)	1.229(5)	1.210(7)	1.227(2)
C2′-Cl/C3′	–	1.750(4)	1.516(4)	–	1.493(7)	1.698(6)	1.510(2)
C1B-O5B	1.420(2)	1.418(4)	1.425(2)	1.402(2)	1.400(5)	1.362(6)	1.402(2)
C5B-O5B	1.442(2)	1.439(5)	1.433(2)	1.436(2)	1.436(2)	1.420(6)	1.444(2)
C6B-O6B	1.420(2)	1.419(5)	1.430(1)	1.426(2)	1.431(5)	1.402(7)	1.431(2)
C4A-C5A-C6A	112.7(1)	113.6(3)	113.4(1)	112.9(1)	112.4(3)	111.4(5)	112.3(3)
O5A-C5A-C6A	106.9(1)	106.8(3)	107.0(1)	106.2(1)	106.1(3)	106.1(4)	106.4(1)
O5A-C1A-N1	107.2 (1)	106.7(3)	107.5(1)	106.5(1)	106.9(3)	105.0(5)	106.7(1)
C2A-C1A-N1	111.4(1)	111.6 (2)	112.3(3)	111.3(1)	112.1(3)	110.7(5)	110.0(1)
N1-C1′-O1′	122.2 (2)	122.8(4)	121.2(1)	122.4(2)	122.1(4)	124.4(6)	122.6(1)
C1′-C2′-Cl/ C3′	–	116.4(3)	111.1(2)	–	110.7(4)	111.2(5)	114.3(1)
C4B-C5B-C6B	112.3(1)	112.3(3)	112.0(2)	111.6(1)	111.5(3)	111.8(5)	110.9(1)
O5B-C5B-C6B	104.5(1)	105.1(3)	106.1 (1)	105.4(1)	105.5(3)	105.5(5)	105.4(1)
C2′-C3′-C4′			113.3(3)				112.4(2)

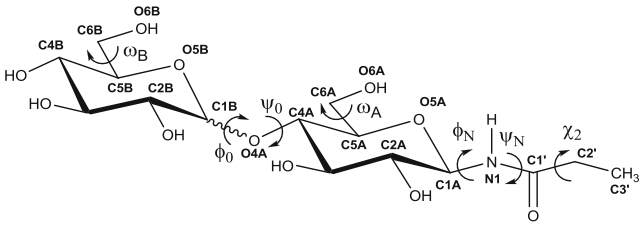

Fig. 4 Depiction of various torsion angles of the *N*-glycoproteins linkage region analogs, ω_B=O5B–C5B–C6B–O6B, ω'_B=C4B–C5B–C6B–O6B, ϕ_O=C4A–O4A–C1B–O5B, Ψ_O=C1B–O4A–C4A–C5A, ω_A=O5A–C5A–C6A–O6A, ω'_A=C4A–C5A–C6A–O6A, ϕ_N=O5A–C1A–N1–C1′, ψ_N=C1A–N1–C1′–C2′ and χ_2=N1–C1′–C2′–C3′

Maltosyl alkanamides (**8–11**)

The molecular packings of the all the maltosyl alkanamides **8**–**11** are also stabilized by extensive networks of hydrogen bonds as well as C–H···O and hydrophobic interactions (Figs. 10 and 11, Tables 8 and 9). As seen earlier with the cellobiosyl alkanamides, all the four maltosyl alkanamides display identical packing features. A finite chain and an infinite chain of hydrogen bonds exist (Table 10). The finite chain starts with N1, runs through O4B, O2W, O3B, O1W and ends at O1′. The infinite chain propagates through O1W, O6A, O2A, O6B, O3A, O2B, and O2W along the crystallographic b-axis (Fig. 11). Intramolecular hydrogen bond between O3A as a donor and O2B as an acceptor is the barrier for rotation around inter glycosidic bond which is observed in other maltosyl derivatives [31]. The two water molecules engage in inter molecular hydrogen bonding leading to the formation of water channels along the crystallographic a-axis (Fig. 12). The acetamido (**8**), propionamido (**9**) and chloroacetamido (**10**) analogs show identical C–H···O interactions (C1A–H1A···O5B & C3B–H3B···O5A). The chloroacetamido analog **10** displays additional C–H···O interaction that makes O1′ a bifurcated acceptor which is also seen for the butanamido analog (**11**). One hydrophobic van der Waals interaction C5A–H5A···H1B–C1B (2.375 Å) is present in the acetamide analog (**8**). Maltosyl analogs (**8**–**11**) are stacked in an antiparallel manner along the crystallographic b-axis.

Conclusions

Parts of the structural data that have been gathered in the present work, bring structural informations which are relevant to the conformational features involved at the *N*-glycosidic linkage in glycoproteins and determines the presentation of the glycan at the protein surface. The question of the effect to distal sugars on the conformation at the *N*-glycosidic linkage was answered through the synthesis and the accurate structural elucidation of several disaccharide alkanamides (**4**–**11**) derived from cellobiose and maltose. Comparisons of crystal structures of synthesized disaccharide analogs with those of previously reported glucosyl analogs (**1**–**3**) showed that the ϕ_N values of cellobiosyl alkanamides (**4**, **6** and **7**) and maltosyl alkanamides (**8**–**11**) exhibit only slight variations (maximum ~9° and ~18°, respectively), with respect to that of GlcβNHAc (**1**). The present work clearly shows that the ϕ_N value deviation by addition of distal sugar through β(1–4) linkage is less as compared to the addition through the α(1–4) linkage. In the case of χ_2 values, a wide range of deviations is seen consistently in the glucosyl, cellobiosyl and maltosyl analogs. This could be ascribed to the greater degree of rotational freedom around C1′-C2′ bond when the C2-NHAc group is absent. This study reveals that the torsion at the *N*-glycosidic linkage can be altered by distal sugars as well as by the nature of the glycosidic linkage (α or β) but to a lesser extent by the structural changes occurring in the aglycon moiety. This demonstrates the structural requirements of *N*-glycosidic linkage region to maintain the linearity, planarity and rigidity which are necessary for *N*-glycan to serve a role in inter- as well as intramolecular protein-carbohydrate interactions. The present investigation brings other structural data that pertain to the area of carbohydrate crystallography, such as the

Table 4 Selected torsion angles of compounds (**1–4 & 6–11**)

Torsion angle	Glucosyl alkanamides			Cellobiosyl alkanamides			Maltosyl alkanamides			
	1	2	3	4	6	7	8	9	10	11
O5B-C5B-C6B-O6B (ω_B)	–	–	–	55.7(2)	54.9(4)	56.0(2)	62.6(2)	62.9(4)	65.2(6)	67.9 (2)
C4B-C5B-C6B-O6B (ω'_B)	–	–	–	175.6(2)	174.8(3)	175.6(2)	−175.8 (1)	−178.2(3)	−172.8(5)	−171.1(2)
C4A-O4A-C1B-O5B (ϕ_O)	–	–	–	−89.3(2)	−90.2(4)	−90.0(2)	102.4(2)	101.8(3)	102.0(5)	102.8(2)
C1B-O4A-C4A-C5A (ψ_O)	–	–	–	−145.9(1)	−145.5(3)	−153.0(1)	−135.5(2)	−134.5(3)	−132.6(5)	−134.4(1)
O5A-C5A-C6A-O6A (ω_A)	−71.8(3)	−69.3(5)	−69.0(4)	−60.8 (2)	−61.0(4)	−59.9(2)	64.6(2)	62.9(4)	63.8(6)	64.4(2)
C4A-C5A-C6A-O6A (ω'_A)	50.1(4)	52.6(5)	51.9(5)	59.8(2)	65.8(4)	61.2(2)	−176.9(2)	−178.2(3)	−179.1(5)	−177.1(2)
O5A-C1A-N1-C1′ (ϕ_N)	−93.7(4)	−89.5(5)	−93.9(4)	−101.8(2)	−101.9(4)	−103.5(2)	−111.5(2)	−109.7(4)	−112.2(6)	−123.4(2)
C1A-N1-C1′-C2′ (ψ_N)	−179.2(3)	166.5(5)	169.9(4)	174..6(2)	175.2(4)	173.0(2)	177.4(2)	−173.8(4)	179.5(6)	−170.3(2)
N1-C1′-C2′-CH_3/Cl (χ_2)	–	114.7	131.3(4)	–	1.6(2)	−100.2(3)	–	−109.9(5)	−133.4(5)	−143.1(2)

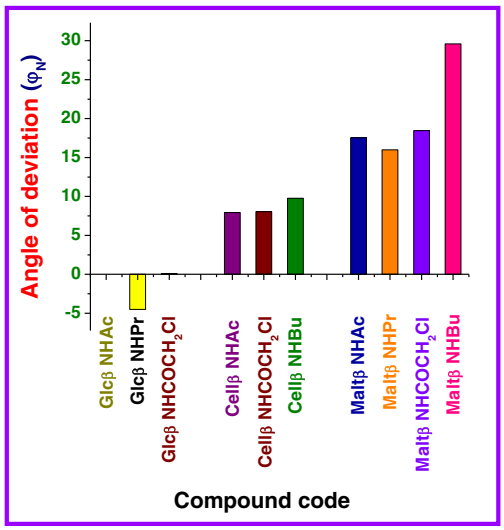

Fig. 5 Graphical representation of variation of ϕ_N values for glucosyl (**1**–**3**), cellobiosyl (**4**, **6** & **7**) and maltosyl (**8**–**11**) alkanamides relative to that of GlcβNHAc (**1**)

relative orientations of the molecules in the crystal lattices, or the occurrence of intermolecular hydrogen bonds, C–H···O and hydrophobic interactions. One value of the present work arises from the possibility to combine the determined features with those recently obtained from low-temperature neutron diffraction series of three *N*-glycoprotein linkage models which provided accurate determination of hydrogen atoms [19]. The results of such an integration will be therefore of interest for testing and improving force fields in order to develop better tools for the modeling of *N*-glycoproteins.

Materials and methods

Materials

All moisture-sensitive reactions were performed under a nitrogen atmosphere using oven-dried glassware. All solvents employed were of commercial grade, purified by distillation and dried according to standard procedures. The dried solvents were stored over 4 Å molecular sieves. All the sugars used were purchased from the Sigma-Aldrich, USA or Carbosynth Limited, UK and used as such without further purification. Thin-layer chromatograms were performed on 25 mm E. Merck silica gel plates (60 F-254). Detection was done by spraying the plates with 10 % sulfuric acid in ethanol and heating on a hot plate. Optical rotations were measured at 30 °C on a JASCO- DIP 200 digital polarimeter using a cell of 10 mm length. NMR spectra were recorded on a Bruker AV400 spectrometer. ESI-MS spectra were measured on a Micromass Q-Tof mass spectrometer.

Methods

Crystal structures resolution and refinement

Crystallization of all the compounds was performed in aqueous methanol by the slow evaporation method at room temperature. X-Ray data collection was performed with a Bruker AXS Kappa Apex II CCD diffractometer equipped with graphite monochromated Mo (Kα) (λ =0.7107 A°) radiation.

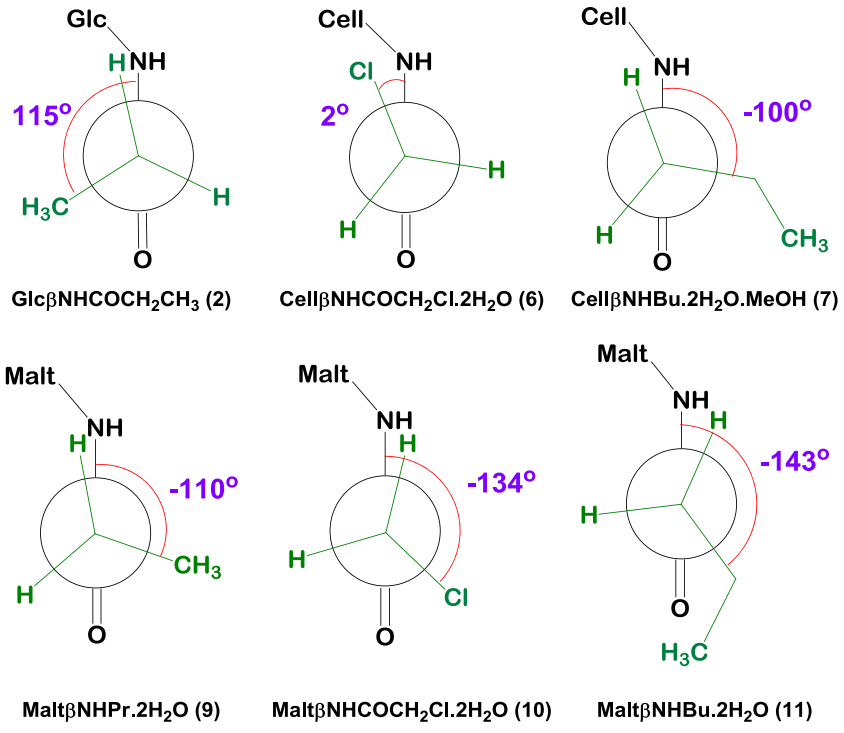

Fig. 6 Newman projections for the variation of side-chain dihedral angle (χ_2) in compounds **2**, **6**, **7**, **9**, **10** and **11**

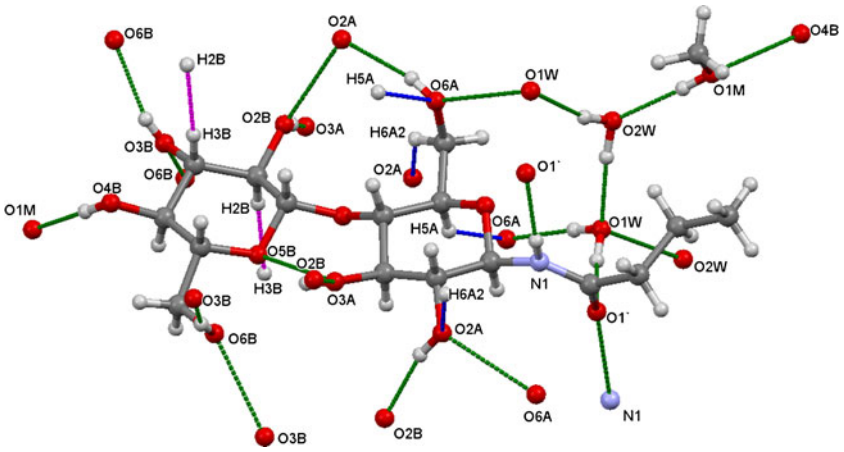

Fig. 7 Non covalent interactions in CellβNHBu.2H_2O.MeOH (**7**) **a** Hydrogen bonds (*green*), **b** C–H · · · O interactions (*blue*), C) Hydrophobic interaction (*magenta*)

A crystal fixed at the tip of a glass fiber was mounted on the goniometer head with the aid of a video microscope. The automatic cell determination routine, with 32 frames at three different orientations of the detector, was employed to collect reflections, and the program APEX2-SAINT [32] was used for finding the unit cell parameters. Fourfold redundancy per reflection was utilized for achieving good absorption correction using multiscan procedure. Besides absorption, Lorentz polarization and decay correction were applied during data reduction. The program SADABS [33] was used for absorption correction using multiscan procedure. The structures were solved by direct methods using SIR92 (WinGX) and refined by full-matrix least-squares techniques using the SHELXL-97 [34] computer program. For compounds **5**–**9** **&** **11**, oxygen and nitrogen H atoms were located in a difference Fourier map and refined isotropically. (All) Other hydrogen atoms were fixed geometrically and allowed to ride on the parent carbon atoms, with aliphatic C-H=0.98\%A and methyl C-H= 0.96\%A. The displacement parameters were set for aliphatic H atoms at U~iso~(H)=1.2U~eq~(C) and for methyl H atoms at 1.5U~eq~(C). The hydrogen belonging to nitrogen and oxygen atoms of compounds **4** and **10** were initially refined with isotropic thermal parameters. The refinement showed some of the hydrogens are refined with bad thermal parameters. Hence, the N-H & O-H hydrogens of compound **4** and O-H hydrogens of compound **10** were geometrically fixed with Fourier peak positions as starting points. O-H distances were fixed at 0.82\%A and were allowed to ride during refinement. Hydrogen atoms of water molecules were located in a difference Fourier map and refined isotropically. Molecular graphics were drawn using ORTEP32 [35] and Mercury programs [36].

The crystal data with refinement details are summarized in Table 11. Complete structural data of the **4**, **6**–**11** have been deposited at the Cambridge Crystallographic Data Centre (CCDC 952466–952472), and can be obtained free of charge via www.ccdc.cam.ac.uk/data_request/cif (or from the Director, Cambridge Crystallographic Data Centre, 12 Union Road, Cambridge CB2 1EZ, UK; fax: +44-1223-336033; or email: deposit@ccdc.cam.ac.uk).

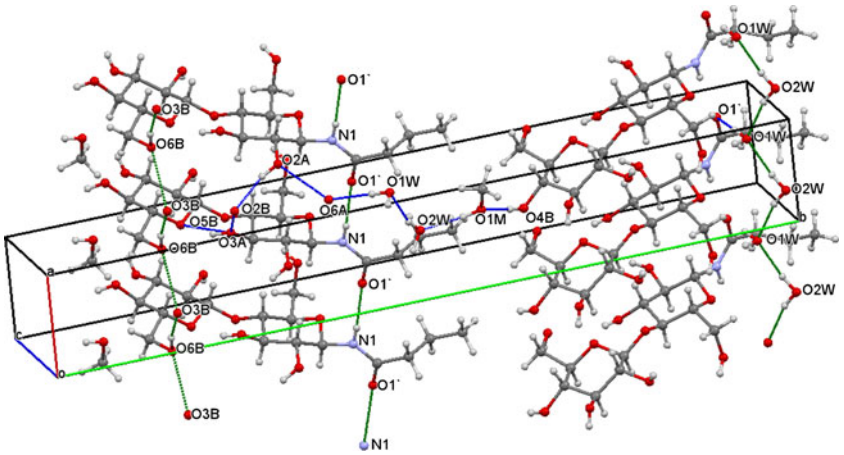

Fig. 8 Molecular packing of CellβNHBu.2H_2O.MeOH (**7**) with finite (*blue*) and infinite (*green*) chain of hydrogen bonds

Table 5 O–H···O and N–H···O hydrogen bonding parameters for cellobiosyl alkanamides (**4**, **6** & **7**)

D–H···A	H···A (Å)	D···A (Å)	D–H···A (°)	Symmetry	H···A (Å)	D···A (Å)	D–H···A (°)	Symmetry	H···A (Å)	D···A (Å)	D–H···A (°)	Symmetry
	Cellβ NHAc.2H_2O (**4**)				Cellβ NHCOCH_2Cl.2H_2O (**6**)				Cellβ NHBu.2H_2O.MeOH (**7**)			
N1–H1N···O1′	2.10(2)	2.884(2)	151.7(1)	1+x, y, z	2.18(4)	2.908(4)	147(4)	−1+x, y, z	1.99(3)	2.819(2)	162(2)	1+x, y, z
O1W–H1W1···O1′	2.18(4)	2.878(3)	157(3)	1+x, y, z	1.95(3)	2.869(5)	169(7)	x, y, z	2.02(4)	2.903(3)	163(3)	x, y, z
O1W–H2W1···O6A	1.92(4)	2.747(2)	167(3)	x, y, z	1.84(2)	2.748(5)	164(6)	1+x, y, z	1.93(4)	2.810(2)	175(3)	−1+x, y, z
O2W–H2W2···O1W	2.08(4)	2.848(3)	171(3)	x, y, z	1.978(3)	2.877(6)	162(4)	2-x, -1/2+y, 1-z	1.95(4)	2.830(3)	170(3)	x, y, z
O2W–H1W2···O1W	1.94(4)	2.767(3)	162(3)	1+x, y, z	2.02(5)	2.793(6)	140(5)	1-x, 1/2+y, 1-z	2.05(4)	2.868(3)	168(3)	1+x, y, z
O2A–H2OA···O2B	1.85(1)	2.6649(3)	173.6(1)	−1+x, 1+y, z	1.87(5)	2.655(4)	162(5)	1+x, y, 1+ z	1.89(3)	2.699(2)	165(2)	−1+x, y, -1+ z
O3A–H3OA···O5B	1.99(1)	2.7506(2)	153.8(1)	x, y, z	1.90(6)	2.765(4)	150(5)	x, y, z	2.02(2)	2.754(2)	151(2)	x, y, z
O6A–H6OA···O2A	1.92(1)	2.7267(2)	168.2(1)	1+x, 1+y, z	2.05(4)	2.764(4)	177(4)	−1+x, y, -1+ z	1.95(2)	2.760(2)	167(2)	1+x, y, -1+ z
O2B–H2OB···O3A	1.95(2)	2.7427(2)	163.1(1)	x, -1+y, z	2.01(4)	2.754(5)	157(4)	x, y, -1+ z	2.05(3)	2.744(2)	178(3)	x, y, 1+ z
O3B–H3OB···O6B	2.07(1)	2.8487(2)	159.5(1)	1+x, -1+y, z	2.14(5)	2.918(5)	154(5)	−1+x, y, -1+ z	2.03(3)	2.772(2)	165(3)	1+x, y, -1+ z
O6B-H6OB···O3B	1.92(2)	2.741(2)	176.9(1)	x, 1+y, z	2.04(6)	2.760(5)	174(6)	x, y, 1+z	1.76(2)	2.719(3)	166(3)	x, y, -1+ z
O4B–H4OB···O2W	1.87	2.684(3)	170.3(1)	1+x, y, -1+ z	1.90(5)	2.704(5)	176(5)	−1+x, y, z	–	–	–	–
O4B–H4OB···O1M	–	–	–	–	–	–	–	–	1.85(4)	2.703(3)	176(3)	1+x, y, 1+ z
O1M–H1OM···O2W	–	–	–	–	–	–	–	–	1.95(4)	2.717(3)	166(4)	1-x,-1/2+y, 1-z

Table 6 C–H···O hydrogen bonding parameters of cellobiosyl alkanamides (**4**, **6** & **7**)

D–H···A	H···A (Å)	D···A (Å)	D–H···A(°)	Symmetry
CellβNHAc.2H_2O (**4**)				
C3A–H3A···O2B	2.683(1)	3.304(2)	121.7(1)	−1+x, 1+y, z
C6B–H6B1···O2W	2.645(2)	3.450(3)	140.6(1)	1+x, y, −1+z
C2B–H2B···O4B	2.647(1)	3.546(2)	152.59(9)	−1+x,y,z
C6A–H6A2···O2A	2.649(2)	3.299(3)	124.7(1)	x, −1+y, z
CellβNHCO$CH_2Cl.2H_2O$ (**6**)				
C2A–H2A···O1′	2.661(3)	3.429(5)	135.4(2)	−1+x, y, z
C3A–H3A···O2B	2.662(3)	3.311(4)	124.0(2)	−1+x, y, z
C6B–H6B1···OW2	2.716(4)	3.415(5)	129.4(3)	−1+x, y, z
C2B–H2B···O4B	2.675(3)	3.592(5)	156.1(2)	1+x, y, z
C6A–H6A2···O2A	2.664(3)	3.292(6)	122.8(2)	x, y, -1+z
CellβNHBu.2H_2O.MeOH (**7**)				
C5A–H5A···O6A	2.564(2)	3.367(3)	139.28	−1+x, y, z
C6A–H6A2···O2A	2.627(2)	3.341(2)	130.66	x, y,1+ z

General procedure for preparation of β-1-N-Alkanamides derived from cellobiose and maltose

The disaccharide (Cellobiose/Maltose) (1 g, 2.9 g) was stirred with saturated ammonium bicarbonate solution for 5 days at room temperature. Solid ammonium bicarbonate was added during the course of the reaction to ensure the saturation. After 5 days, the solution was lyophilized twice. Excess ammonium bicarbonate was removed by extracting the glycosylamine in dry methanol followed by filtration. Concentration of the methanolic solution to dryness gave the glycosylamine as a solid. Crude glycosylamine was dissolved in dry methanol (15 mL) and cooled to 0 °C. To this solution anhydride (4.4 mmol) was added, in portions and the reaction mixture was stirred for 2 h at 0 °C, followed by stirring at room temperature overnight. The precipitated solid from the solution was filtered and washed with cold methanol. The resultant white solid was recrystallized from aqueous methanol.

N-{(4-*O*-β-D-Glucopyranosyl)-β-D-glucopyranosyl}-acetamide (**4**):

Yield 0.35 g (30 %); crystalline solid; mp 150–152 °C; $[\alpha]_D^{30}$ -11.6° (c 1, H_2O); IR (neat, cm^{-1}): 3290, 2880, 1644, 1540, 1472, 1451, 1421, 1362, 1317, 1291, 1257, 1167, 1153, 1116, 1076, 1026, 993, 954, 902, 889, 636; ^{1}H NMR (400 MHz, D_2O): δ 5.01 (d, 1H, *J*=9.2 Hz, H-1a), 4.55 (d, 1H, *J*=8.0 Hz, H-1b), 4.00–3.93 (m, 2H), 3.89–3.82 (m, 1H), 3.81–3.67 (m, 4H), 3.58–3.42 (m, 4H), 3.40–3.33 (m, 1H), 2.11 (s, 3H, CH_3); ^{13}C NMR (100 MHz, D_2O): δ 175.5 (CO), 102.6 (C-1b), 79.1 (C-1a), 76.4, 76.0, 75.5, 75.0, 74.3, 73.1, 71.6, 69.5, 60.7,

Table 7 Finite and infinite chain of H-bonding in cellobiosyl alkanamides (**4**, **6** & **7**)

Compound code and no.	Finite chain of H-bonding	Infinite chain of H-bonding
CellβNHAc.	N1−H1N- O1′	···O6B–H6OB···
2H_2O (**4**)	O4B–H4OB···O2W–H1W2···O1W–H2W1···O1′	O3B–H3OB···
	O4B–H4OB···O2W–H1W2···O1W–H2W1···O6A–H6OA··· O2A–H2OA···O2B–H2OB···O3A–H3OA···O5B	
CellβNHCO	N1−H1N- O1′	···O6B–H6OB···
$CH_2Cl.2H_2O$ (**6**)	O4B–H4OB···O2W–H1W2···O1W–H2W1···O1′	O3B–H3OB···
	O4B–H4OB···O2W–H1W2···O1W–H2W1···O6A–H6OA··· O2A–H2OA···O2B–H2OB···O3A–H3OA···O5B	
CellβNHBu.	N1−H1N- O1′	···O6B–H6OB···
2H_2O.MeOH (**7**)	O4B–H4OB···O2W–H1W2···O1W–H2W1···O1′	O3B–H3OB···
	O4B–H4OB···O1M–H1OM···O2W–H1W2··· O1W–H2W1···O6A–6OA···O2A–H2OA···O2B–2OB··· O3A–H3OA···O5B	

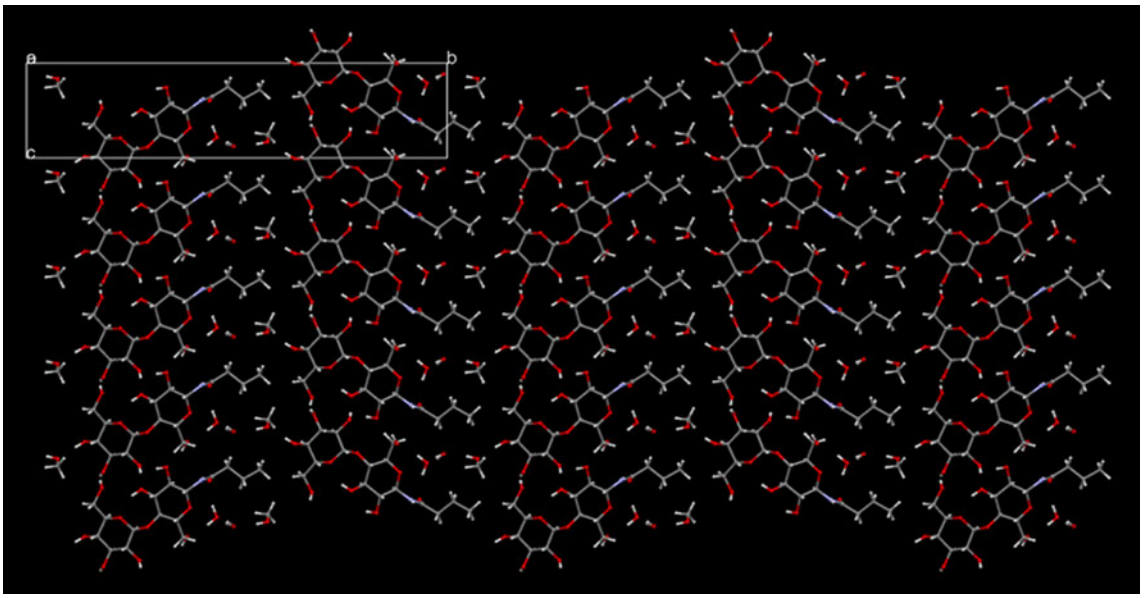

Fig. 9 Crystal packing of CellβNHBu.2H_2O.MeOH (**7**) projected along a-axis

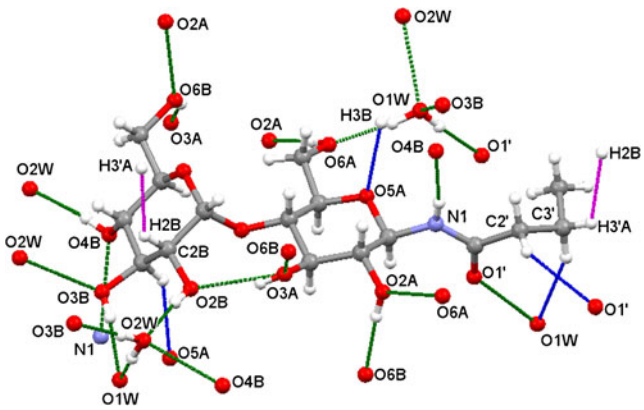

Fig. 10 Non covalent interactions in MaltβNHBu.2H_2O (**11**) **a** Hydrogen bonds (*green*), **b** C–H···O interactions (*blue*), **c** Hydrophobic interaction (*magenta*)

59.9, 22.6 (−$\underline{C}H_3$); ESI-MS: calcd for $C_{14}H_{25}NO_{11}Na$ ($[M+Na]^+$): 406.1325. found: 406.1329.

N-{(4-*O*-β-D-Glucopyranosyl)-β-D-glucopyranosyl}-propionamide (**5**):

Yield 0.35 g (29 %); white solid; mp 103–106 °C; $[\alpha]_D^{30}$ -12.6° (c 1, H_2O); IR (neat, cm^{-1}): 3209, 1665, 1650, 1568, 1422, 1355, 1302, 1170, 1112, 1076, 1053, 1036, 1020, 991, 913, 705, 633, 615; ^1H NMR (400 MHz, D_2O): δ 4.92 (d, 1H, *J*=9.2 Hz, H-1a), 4.46 (d, 1H, *J*=8.0 Hz, H-1b), 4.00–3.55 (m, 7H), 3.50–3.20 (m, 5H), 2.27 (q, 2H, $C\underline{H}_2CH_3$), 1.06 (t, 2H, $CH_2C\underline{H}_3$); ^{13}C NMR (100 MHz, D_2O): δ 179.3 (CO), 102.5 (C-1b), 79.1 (C-1a), 78.1.0, 76.4, 76.0, 75.5, 75.0, 73.2, 71.6, 69.5, 60.6, 59.9, 29.1 (−$\underline{C}H_2CH_3$), 9.1 (−$CH_2\underline{C}H_3$); ESI-MS: calcd for $C_{15}H_{27}NO_{11}Na$ ($[M+Na]^+$): 420.1482. found: 420.1485.

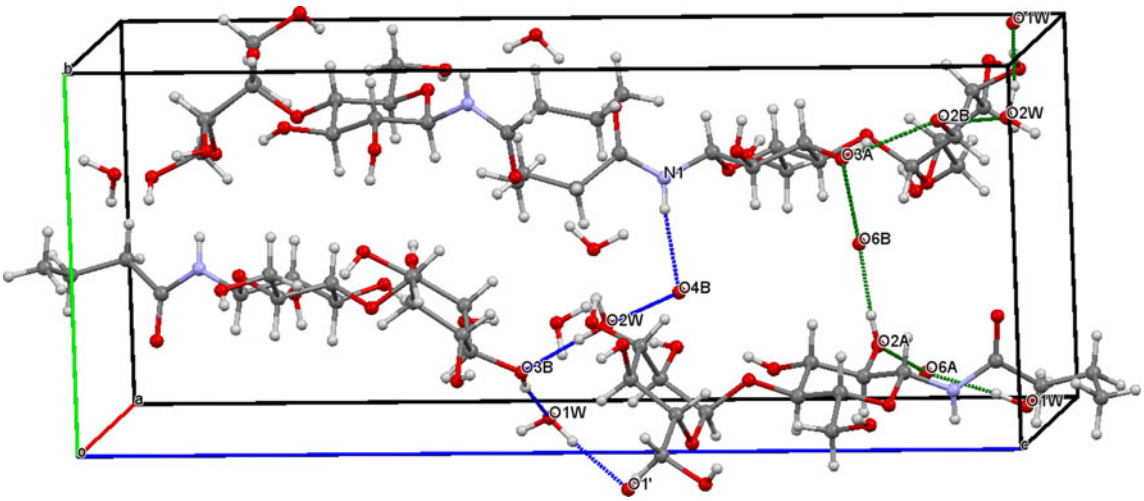

Fig. 11 Molecular packing of MaltβNHBu.2H_2O (**11**) with finite (*blue*) and infinite (*green*) chain of hydrogen bonds

Table 8 O–H···O and N–H···O hydrogen bonding parameters for maltosyl alkanamides (**8**–**11**)

D–H···A	H···A (Å)	D···A (Å)	D–H···A(°)	Symmetry	H···A (Å)	D···A (Å)	D–H···A(°)	Symmetry
	MaltβNHAc.2H_2O (**8**)				MaltβNHPr.2H_2O (**9**)			
N1–H1N···O4B	2.11(3)	2.927(2)	160(2)	1-x, 1/2+y, 3/2-z	2.09(7)	2.942(5)	162(5)	2-x, -1/2+y, 3/2-z
O1W–H1W1···O1′	1.83(3)	2.694(2)	177(3)	x, y, z	1.84(4)	2.696(4)	178(4)	1/2+x, 1/2-y, 1-z
O6A–H6OA···O2A	1.82(3)	2.672(2)	173(3)	−1+x, y, x	1.81(4)	2.671(5)	176(5)	1+x, y, x
O2A–H2OA···O6B	1.86(3)	2.672(2)	172(3)	1-x, 1/2+y, 3/2-z	1.88(4)	2.675(4)	156(5)	2-x, 1/2+y, 3/2-z
O6B–H6OB···O3A	1.91(3)	2.690(2)	173(3)	−1+x, y, z	1.86(5)	2.685(5)	167(4)	1+x, y, x
O3A–H3OA···O2B	1.96(3)	2.731(2)	175(3)	x, y, z	1.80(5)	2.735(4)	159(5)	x, y, z
O1W–H2W1···O6A	1.83(3)	2.712(2)	174(3)	1/2+x, 1/2-y, 1-z	1.90(3)	2.720(5)	164(5)	x, y, z
O2B–H2OB···O2W	1.97(2)	2.7124(2)	169(2)	x, y, z	1.94(4)	2.713(5)	167(4)	x, y, z
O3B–H3OB···O1W	1.97(2)	2.760(2)	171(2)	3/2-x, -y, 1/2+z	1.89(6)	2.751(5)	162(5)	2-x, 1/2+y, 3/2-z
O2W–H2W2···O3B	1.94(3)	2.7226(2)	176(2)	1/2+x, 1/2-y, 1-z	1.87(4)	2.729(5)	173(7)	−1/2+x, 1/2-y, 2-z
O2W–H1W2···O1W	1.81(3)	2.701(2)	168(3)	1.5-x, -y, 1/2+z	1.88(6)	2.701(5)	161(5)	2-x, 1/2+y, 3/2-z
O4B–H4OB···O2W	1.92(3)	2.745(2)	170(3)	−1+x, y, z	1.81(5)	2.739(5)	172(4)	1+x, y, z
	MaltβNHCOCH_2Cl.2H_2O (**10**)				MaltβNHBu.2H_2O (**11**)			
N1–H1N···O4B	2.04(6)	2.885(7)	169(5)	-x+1, y+1/2,-z+1/2	2.20(2)	3.0003(2)	170.7(2)	2-x, -1/2+y, 3/2-z
O1W–H1W1···O1′	1.87(6)	2.710(6)	169(7)	x-1/2,-y+3/2,-z	1.904(2)	2.7495(2)	173(2)	1/2+x, 3/2-y, 1-z
O6A–H6OA···O2A	1.823(4)	2.634(6)	169(5)	-x+1,y,z	1.916(2)	2.726(2)	172(2)	1+x, y, z
O2A–H2OA···O6B	2.085(4)	2.622(5)	123.0(3)	1-x, -1/2+y, 1/2-z	1.89(2)	2.7026(2)	176(2)	2-x, 1/2+y, 3/2-z
O6B–H6OB···O3A	1.900(4)	2.664(6)	154(8)	−1+x, y, z	1.95(2)	2.7345(2)	158.1(2)	1+x, y, z
O3A–H3OA···O2B	1.885(4)	2.693(5)	168.6(3)	x, y, z	2.01(2)	2.7492(2)	163(2)	x, y, z
O1W–H2W1···O6A	1.84(4)	2.674(6)	166(6)	x, y, z	1.898(2)	2.7494(2)	174(2)	x, y, z
O2B–H2OB···O2W	1.901(4)	2.674(6)	156.6(3)	x, y, z	1.906(2)	2.730(2)	173(2)	x, y, z
O3B–H3OB···O1W	1.955(5)	2.737(6)	159.0(3)	1-x, -1/2+y, 1/2-z	1.98(2)	2.7554(2)	169(2)	2-x, 1/2+y, 3/2-z
O2W–H2W2···O3B	1.86(4)	2.692(6)	165(6)	1/2+x, 3/5-y,1-z	1.90(2)	2.7213(2)	158(2)	2-x, 1/2+y, 3/2-z
O2W–H1W2···O1W	1.86(6)	2.680(7)	159(6)	1-x,-1/2+y,1/2-z	1.87(2)	2.7364(2)	177(3)	−1/2+x, 3/2-y, 2-z
O4B–H4OB···O2W	1.870(4)	2.668(6)	163.7(3)	−1+x,y,z	1.94(2)	2.7578(2)	169(2)	1+x, y, z

N-{(4-*O*-β-D-Glucopyranosyl)-β-D-glucopyranosyl}-chloroacetamide (**6**):

Yield 0.34 g (27 %); crystalline solid; mp 130–132 °C; $[\alpha]_D^{30}$ −12.2° (c 1, H_2O); IR (neat, cm^{-1}): 3279, 2871, 2362,

Table 9 C–H···O hydrogen bonding parameters of maltosyl alkanamides (**8**–**11**)

D–H···A	H···A (Å)	D···A (Å)	D–H···A(°)	Symmetry
MaltβNHAc.2H_2O (**8**)				
C1A–H1A···O5B	2.60(2)	3.494(2)	157(1)	1-x, −1/2+y, 3/2-z
C3B–H3B···O5A	2.55(2)	3.346(2)	138(1)	1-x, -1/2+y, 3/2-z
MaltβNHPr.2H_2O (**9**)				
C1A–H1A···O5B	2.62(5)	3.544(5)	156(4)	2-x, 1/2+y , 3/2-z
C3B–H3B···O5A	2.55(4)	3.348(5)	143(3)	2-x, 1/2+y , 3/2-z
MaltβNHCOCH_2Cl.2H_2O (**10**)				
C2′–H2′A···O1′	2.587(5)	3.551(8)	172.5(4)	1/2+x, 3/2-y, -z
C1A–H1A···O5B	2.561(4)	3.492(7)	158.8(3)	1-x,-1/2+y,1/2-z
C3B–H3B···O5A	2.467(4)	3.292(7)	141.7(3)	1-x,-1/2+y,1/2-z
MaltβNHBu.2H_2O (**11**)				
C2′–H2′B···O1′	2702(1)	3.530(2)	143.6(1)	−1/2+x, 3/2-y, 1-z
C3B–H3B···O5A	2.53(2)	3.343(2)	142(1)	2-x, 1/2+y, 3/2-z

Table 10 Finite and infinite chain of hydrogen bonding in maltosyl alkanamides (**8**–**11**)

Compound code and no.	Finite chain of H-bonding	Infinite chain of H-bonding
MaltβNHAc. $2H_2O$ (**8**)	N1-H1N···O4B–H4OB···O2W–H2W2···O3B–H3OB···O1W–H1W1···O1′	···O1W–H2W1···O6A–H6OA···O2A–H2OA···O6B–H6OB···O3A–H3OA···O2B–H2OB···O2W–H1W2···O1W–
MaltβNHPr. $2H_2O$ (**9**)	N1-H1N···O4B–H4OB···O2W–H2W2···O3B–H3OB···O1W–H1W1···O1′	···O1W–H2W1···O6A–H6OA···O2A–H2OA···O6B–H6OB···O3A–H3OA···O2B–H2OB···O2W–H1W2···O1W–
MaltβNHCO $CH_2Cl.2H_2O$ (**10**)	N1-H1N···O4B–H4OB···O2W–H2W2···O3B–H3OB···O1W–H1W1···O1′	···O1W–H2W1···O6A–H6OA···O2A–H2OA···O6B–H6OB···O3A–H3OA···O2B–H2OB···O2W–H1W2···O1W–
MaltβNHBu. $2H_2O$ (**11**)	N1-H1N···O4B–H4OB···O2W–H2W2···O3B–H3OB···O1W–H1W1···O1′	···O1W–H2W1···O6A–H6OA···O2A–H2OA···O6B–H6OB···O3A–H3OA···O2B–H2OB···O2W–H1W2···O1W–

1637, 1541, 1468, 1448, 1406, 1358, 1318, 1290, 1264, 1169, 1151, 1115, 1076, 1059, 1047, 1036, 994, 955, 927, 902, 891, 792, 634, 559, 514; ^{1}H NMR (400 MHz, D_2O): δ 5.03 (d, 1H, J=9.2 Hz, H-1A), 4.51 (d, 1H, J=7.9 Hz, H-1B), 4.20 (s, 2H, $C\underline{H}_2Cl$), 3.98–3.87 (m, 2H), 3.86–3.78 (m, 1H), 3.77–3.62 (m, 4H), 3.54–3.36 (m, 4H), 3.31 (t, J=8.8 Hz, 1H); ^{13}C NMR (100 MHz, D_2O): δ 170.8 (CO), 102.5 (C1-b), 79.4 (C-1a), 77.9, 76.4, 75.4, 75.9, 75.4, 74.8, 73.1, 71.4, 69.4, 60.5, 59.7, 42.2 ($-\underline{C}H_2Cl$); ESI-MS: calcd for $C_{14}H_{24}NO_{11}NaCl$ ($[M+Na]^+$): 440.0936. found: 440.0929.

N-{(4-*O*-β-D-Glucopyranosyl)-β-D-glucopyranosyl}-butanamide (**7**):

Yield 0.56 g (43 %); crystalline solid; mp 144–147 °C; $[\alpha]_D^{30}$ −13.4° (c 1, H_2O); IR (neat, cm^{-1}): 3242, 2930, 2884, 1654, 1564, 1448, 1362, 1294, 1257, 1225, 1170, 1074, 1017, 985, 903, 595, 577, 533; ^{1}H NMR (400 MHz, D_2O): δ 5.02 (d, 1H, J=9.2 Hz, H-1a), 4.56 (d, 1H, J=8.0 Hz, H-1b), 4.01–3.67 (m, 2H), 3.58–3.32 (m, 5H), 2.34 (t, 2H, J=7.6 Hz, -$C\underline{H}_2CH_2CH_3$), 1.67 (m, 2H, -$CH_2C\underline{H}_2CH_3$), 0.96 (t, 3H, J= 7.2 Hz, -$CH_2CH_2C\underline{H}_3$); ^{13}C NMR (100 MHz, D_2O): δ 178.6 (CO), 102.6 (C-1b), 79.1 (C-1a), 78.3, 76.4, 76.1, 75.6, 75.1, 73.2, 71.6, 69.6, 60.7, 60.0, 37.7 ($-\underline{C}H_2CH_2CH_3$), 18.7 ($-CH_2\underline{C}H_2CH_3$), 12.8 ($-CH_2CH_2\underline{C}H_3$); ESI-MS: calcd for $C_{16}H_{29}NO_{11}Na$ ($[M+Na]^+$): 434.1638. found: 434.1642.

N-{(4-*O*-α-D-Glucopyranosyl)-β-D-glucopyranosyl}-acetamide (**8**):

Yield 0.41 g (36 %); crystalline solid; mp 116–118 °C; $[\alpha]_D^{30}$ 75.9° (c 1, H_2O); IR (neat, cm^{-1}): 3224, 2941, 2903, 1665, 1572, 1376, 1341, 1299, 1149, 1118, 1075, 1027, 954, 918, 840, 788, 709, 673; ^{1}H NMR (400 MHz, D_2O): δ 5.43 (d, 1H, J=3.8 Hz, H-1b), 4.97 (d, 1H, J=9.2 Hz, H-1a), 3.93–3.65 (m, 9H), 3.59 (dd, J=4, 10 Hz, 1H), 3.43 (t, J=9.2 Hz, 2H), 2.08 (s, 3H, -$C\underline{H}_3$); ^{13}C NMR (100 MHz, D_2O): δ 175.5 (CO), 99.6 (C-1b), 79.1 (C-1a), 76.9, 76.2, 76.1, 72.9, 72.7, 71.7, 71.6, 69.3, 60.5, 22.1 ($-\underline{C}H_3$); ESI MS: calcd for $C_{14}H_{25}NO_{11}Na$ ($[M+Na]^+$): 406.1325. found: 406.1316.

N-{(4-*O*-α-D-Glucopyranosyl)-β-D-glucopyranosyl}-propionamide (**9**):

Yield 0.62 g (53 %); crystalline solid; mp 119–120 °C; $[\alpha]_D^{30}$ 76.1° (c 1, H_2O); IR (neat, cm^{-1}): 3252, 1660, 1567, 1372, 1342, 1149, 1115, 1076, 1024, 995, 910, 841, 788, 699; ^{1}H NMR (400 MHz, D_2O): δ 5.43 (d, 1H, J=3.8 Hz, H-1b), 4.97 (d, 1H, J=9.2 Hz, H-1a), 3.93–3.64 (m, 9H), 3.57 (dd, J=4, 10 Hz, 1H), 3.46–3.38 (m, 2H), 2.34 (q, 2H, J=7.6 Hz, -$C\underline{H}_2CH_3$), 1.13 (t, 3H, J=7.6 Hz, -$CH_2C\underline{H}_3$); ^{13}C NMR (D_2O, 100 MHz): δ 176.9 (CO), 97.1 (C1b), 76.6 (C1a), 74.5, 73.7, 70.4, 70.2, 69.2, 69.1, 66.8, 58.0, 57.9, 26.6

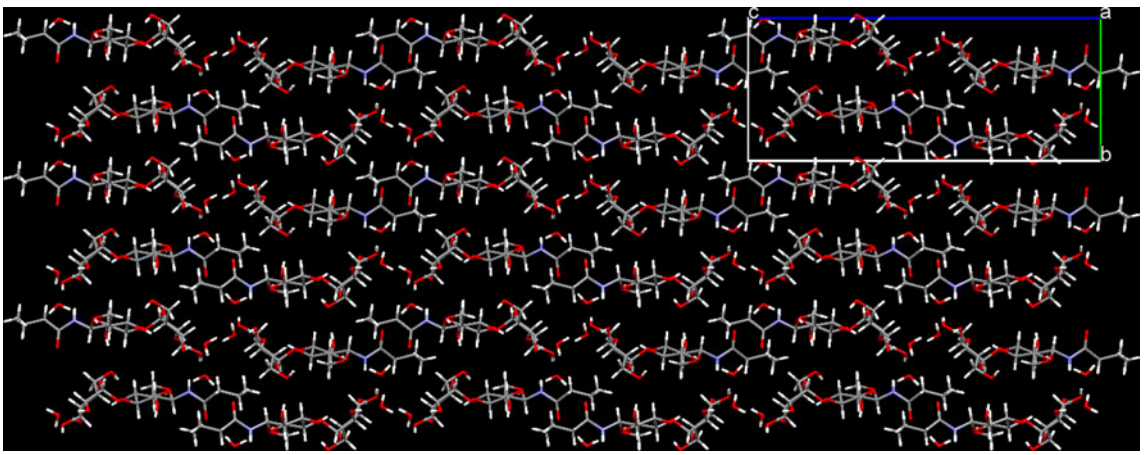

Fig. 12 Crystal packing of MaltβNHBu.$2H_2O$ (**11**) projected along a-axis

Table 11 Data Collection and refinement statistics of disaccharide alkanamides (**4 & 6–11**)

Parameter	CellβNHAc. $2H_2O$ (**4**)	CellβNHCO $CH_2Cl.2H_2O$ (**6**)	CellβNHBu. $2H_2O$.MeOH (**7**)	MaltβNHAc. $2H_2O$ (**8**)	MaltβNHPr. $2H_2O$ (**9**)	MaltβNHCO $CH_2Cl.2H_2O$ (**10**)	MaltβNHBu. $2H_2O$ (**11**)
Empirical Formula	C_{14} H_{29} N O_{13}	C_{14} H_{28} Cl N O_{13}	C_{17} H_{37} N O_{14}	$C_{14}H_{29}NO_{13}$	C_{15} H_{31} N O_{13}	C_{14} H_{28} Cl N O_{13}	C_{16} H_{33} N O_{13}
Formula weight	419.38	453.82	479.48	419.38	433.41	453.82	447.43
Wavelength	0.71073 Å	0.71073 Å	0.71073 Å	0.71073 Å	0.71073 Å	0.71073 Å	0.71073 Å
Crystal system	Triclinic	Monoclinic	Monoclinic	Orthorhombic	Orthorhombic	Orthorhombic	Orthorhombic
Space group	$P1$	$P2_1$	$P2_1$	$P2_12_12_1$	$P2_12_12_1$	$P2_12_12_1$	$P2_12_12_1$
Cell Dimensions	a=5.004(2) b=7.625(2) c=12.934(5) α=89.40(2) β=86.67(2) γ=73.95(4)	a=5.107(5) b=26.165(3) c=7.6431(9) α=90 β=106.76(4) γ=90	a=4.885(10) b=32.488(11) c=7.555(3) α=90 β=103.80(10) γ=90	a=8.7305(5) b=9.6012(4) c=24.6747(12) α=90.00 β=90.00 γ=90.0	a=8.687(12) b=9.660(13) c=24.785(3) α=90 β=90 γ=90	a=8.4700(17) b=9.5840(19) c=24.540(5) α=90 β=90 γ=90	a=8.6133(7) b=10.0113(7) c=24.7143(19) α=90 β=90 γ=90.
Volume ($Å^3$)	473.46(3)	977.91(19)	1164.50(7)	2068.31	2079.8(5)	1992.1(7)	2131.1(3)
Z, calculated density (Mg/m^3)	1, 1.471	2, 1.541	2, 1.367	4, 1.347	4, 1.346	4, 1.513	4, 1.395
Absorption coefficient (mm^{-1})	0.131	0.266	0.119	0.120	0.122	0.261	0.121
F(000)	224	480	516	896	904	960	960
Crystal size (mm)	0.23×0.19×0.15	0.35×0.01×0.01	0.38×0.25×0.22	0.32×0.22×0.20	0.58×0.31×0.17	0.35×0.09×0.09	0.11×0.10×0.10
Theta range (°)	3.16 to 28.28	3.11 to 25.16	2.51 to 29.25	2.28 to 28.28	1.64 to 25.00	2.28 to 28.46	2.19 to 28.24
Index ranges	−5<=h<=6 −9<=k<=10 −17<=l<=17	−5<=h<=5 −30<=k<=31 −9<=l<=9	−4<=h<=6 −38<=k<=43 −9<=l<=9	−11<=h<=11 −12<=k<=11 −32<=l<=32	−10<=h<=10 −11<=k<=8 −28<=l<=29	−11<=h<=11 −12<=k<=11 −22<=l<=32	−11<=h<=11 −12<=k<=12 −32<=l<=32
Reflections collected / unique	6106/3566 [R(int)=0.0179]	5417 / 2609 [R(int)=0.0375]	8225 / 4398 [R(int)=0.0155]	23650 / 5019 [R(int)=0.0467]	21937 / 3666 [R(int)=0.1278]	11208 / 4699 [R(int)=0.1026]	29096 / 5080 [R(int)=0.0388]
Data / restraints / parameters	3566 / 3 / 277	2609 /7 / 310	4398 / 1 / 343	5019 / 0 / 359	3666 / 9 / 355	4699 / 6/ 284	5080 / 6 / 360
Goodness-of-fit on F^2	1.038	1.039	1.410	1.033	1.053	0.946	1.021
Final R indices [I > 2sigma(I)]	R1=0.0301 wR2=0.0812	R1=0.0393 wR2=0.0792	R1=0.0347 wR2=0.0727	R1=0.0396 wR2=0.0887	R1=0.0584 wR2=0.1382	R1=0.0737 wR2=0.1246	R1=0.0351 wR2=0.0681
R indices (all data)	R1=0.0318 wR2=0.0825	R1=0.0550 wR2=0.0853	R1=0.0392 wR2=0.0743	R1=0.0492 wR2=0.0934	R1=0.0802 wR2=0.1522	R1=0.2253 wR2=0.1748	R1=0.0491 wR2=0.0727

(−$\underline{C}H_2CH_3$), 6.6 (−$CH_2\underline{C}H_3$); ESI MS: calcd for $C_{16}H_{29}NO_{11}Na$ ([M+Na]$^+$): 420.1482. found: 420.1489.

N-{(4-*O*-α-D-Glucopyranosyl)-β-D-glucopyranosyl}-chloroacetamide (**10**):

Yield 0.43 (35 %); crystalline solid; mp 125–128 °C; $[\alpha]_D^{30}$ 76.9° (c 1, H_2O); IR (neat, cm^{-1}): 3231, 1682, 1581, 1430, 1374, 1340, 1305, 1149, 1114, 1075, 1026, 1006, 957, 881, 840, 789, 703, 618; ^{1}H NMR (400 MHz, D_2O): δ 5.47 (d, 1H, *J*=3.8 Hz, H-1b), 5.08 (d, 1H, *J*=9.2 Hz, H-1a), 4.26 (s, 2H, -$C\underline{H}_2$Cl), 3.98–3.70 (m, 9H), 3.63 (dd, *J*=4, 10 Hz, 1H), 3.53 (t, *J*=9.2 Hz), 3.47 (t, *J*=9.6 Hz, 1H); ^{13}C NMR (D_2O, 100 MHz): δ 170.9 (CO), 99.7 (C-1B), 79.5 (C-1A), 76.9, 72.9, 72.8, 71.8, 71.6, 69.4, 60.6, 42.3 ($\underline{C}H_2$Cl); ESI MS: calcd for $C_{14}H_{24}NO_{11}Na$ ([M + Na]$^+$): 440.0936. found: 440.0939.

N-{(4-*O*-α-D-Glucopyranosyl)-β-D-glucopyranosyl}-butanamide (**11**):

Yield 0.54 g (44 %); crystalline solid; mp 85–86 °C; $[\alpha]_D^{30}$ 76.5° (c 1, H_2O); IR (neat, cm^{-1}): 3259, 1664, 1568, 1425, 1374, 1339, 1279, 1146, 1115, 1072, 1022, 995, 948, 841, 698, 628; ^{1}H NMR (400 MHz, D_2O): δ 5.44 (d, 1H, *J*=3.6 Hz, H-1b), 4.99 (d, 1H, *J*=9.2 Hz, H-1a), 3.95–3.64 (m, 9H), 3.60 (dd *J*=4, 10 Hz, 1H), 3.44 (t, *J*=9.2 Hz, 2H), 2.32 (t, 2H, *J*=7.6 Hz, -$C\underline{H}_2CH_2CH_3$), 1.65 (m, 2H, -$CH_2C\underline{H}_2CH_3$), 0.94 (t, 3H, *J*=7.6 Hz, -$CH_2CH_2C\underline{H}_3$); ^{13}C NMR (D_2O, 100 MHz): δ 178.6 (CO), 99.7 (C-1b), 79.2 (C-1a), 77.0, 76.5, 76.3, 73.0, 72.8, 71.8, 71.7, 69.5, 60.7, 60.6, 37.8 (−$\underline{C}H_2CH_2CH_3$), 18.8 (−$CH_2\underline{C}H_2CH_3$), 12.8 (−$CH_2CH_2\underline{C}H_3$); ESI MS: calcd for $C_{16}H_{29}NO_{11}Na$ ([M + Na]$^+$): 434.1638. found: 434.1651.

Acknowledgments We are grateful to the Indo-French Centre for Promotion of Advanced Research (IFCPAR), New Delhi, for the financial support and encouragement. Funding provided by the Department of Science and Technology, New Delhi, for the purchase of the 400 MHz NMR under IRHPA Scheme and ESI-MS under the FIST program to the Department of Chemistry, IIT Madras is gratefully acknowledged. We are thankful to Dr. Babu Varghese for discussions and technical help. One of us (M.M.) is thankful to the Council of Scientific and Industrial Research (CSIR), New Delhi, for award of a Senior Research Fellowship. We also thank Cambridge Crystallographic Data Centre (CCDC), United Kingdom, for making the program Mercury 3.0 available for use.

References

1. Dwek, R.A.: Glycobiology: toward understanding the function of sugars. Chem. Rev. **96**, 683–720 (1996)
2. Gabius, H.J., Siebert, H.C., Andre, S., Jimenez-Barbero, J., Rudiger, H.: Chemical biology of the sugar code. Chembiochem **5**, 740–764 (2004)
3. Varki, A.: Biological roles of oligosaccharides: all of the theories are correct. Glycobiology **3**, 97–130 (1993)
4. Varki, A., Cummings, R., Esko, J., Freeze, H., Hart, G., Marth, J.: Essentials of Glycobiology. Cold Spring Harbor Laboratory Press, Cold Spring Harbor (1999)
5. Spiro, R.G.: Protein glycosylation: nature, distribution, enzymatic formation, and disease implication of glycopeptide bonds. Glycobiology **12**, 43R–56R (2002)
6. Lee, K.C., Falcone, M.L., Davis, J.T.: Sequence-specific peptide-carbohydrate interactions in an asparagine-linked glycopeptide. J. Org. Chem. **61**, 4198–4199 (1996)
7. O'Connor, S.E., Pohlmann, J., Imperiali, B., Saskiwan, I., Yamamoto, K.: Probing the effect of the outer saccharide residues of *N*-linked glycans on peptide conformation. J. Am. Chem. Soc. **123**, 6187–6188 (2001)
8. Bosques, C.J., Tschampel, S.M., Wood, R.J., Imperiali, B.: Effects of glycosylation on peptide conformation: a synergistic experimental and computational study. J. Am. Chem. Soc. **126**, 8421–8425 (2004)
9. O'Connor, S.E., Imperiali, B.: A molecular basis for glycosylation-induced conformational switching. Chem. Biol. **5**, 427–437 (1998)
10. Sriram, D., Srinivasan, H., Srinivasan, S., Priya, K., Vishnu Thirtha, M., Loganathan, D.: β-1-*N*-Acetamido-D-glucopyranose. Acta Crystallogr. **C53**, 1075–1077 (1997)
11. Sriram, D., Lakshmanan, T., Loganathan, D., Srinivasan, S.: Crystal structure of a hydrated *N*-glycoprotein linkage region model and its analogue: hydrogen bonding and Pi-Pi stacking driven molecular assembly. Carbohydr. Res. **309**, 227–236 (1998)
12. Aich, U., Lakshmanan, T., Varghese, B., Loganathan, D.: Crystal structures of β-1-*N*-chloroacetamido derivatives of D-glucose and D-galactose. J. Carbohydr. Chem. **22**, 891–901 (2003)
13. Lakshmanan, T., Sriram, D., Priya, K., Loganathan, D.: On the structural significance of GlcNAc and Asn as the linkage region constituents in *N*-glycoproteins: a crystallographic investigation using models and analogs. Biochem. Biophys. Res. Commun. **312**, 405–413 (2003)
14. Loganathan, D., Aich, U., Lakshmanan, T.: Chemoenzymatic synthesis and X-ray crystallographic investigation of *N*-glycoprotein linkage region models and analogs. Proc. Indian Nat. Sci. Acad. **71A**, 213–236 (2005)
15. Mohamed Naseer Ali, M., Aich, U., Varghese, B., Pérez, S., Imberty, A., Loganathan, D.: Conformational preferences of the aglycon moiety in models and analogs of GlcNAc-Asn linkage: crystal structures and ab initio quantum chemical calculations of *N*-(−D-glycopyranosyl)haloacetamides. J. Am. Chem. Soc. **130**, 8317–8325 (2008)
16. Mohamed Naseer Ali, M., Aich, U., Varghese, B., Pérez, S., Imberty, A., Loganathan, D.: Examination of the effect of structural variation on the *N*-glycosidic torsion (ϕ_N) among *N*-(β-D-glycopyranosyl)acetamido and propionamido derivatives of monosaccharides based on crystallography and quantum chemical calculations. Carbohydr. Res. **344**, 355–361 (2009)
17. Mathiselvam, M., Varghese, B., Loganathan, D.: Synthesis and X-ray crystallographic investigation of *N*-(3-deoxy-3-acetamido-β-D-glycopyranosyl)alkanamides as analogs of *N*-glycoprotein linkage region. Glycoconj. J. **28**, 573–580 (2011)
18. Loganathan, D., Aich, U.: Observation of a unique pattern of bifurcated hydrogen bonds in the crystal structures of the *N*-glycoprotein linkage region models. Glycobiology **16**, 343–348 (2006)
19. Cioci, G., Srivastava, A., Loganathan, D., Mason, S.A., Pérez, S., Imberty, A.: Low temperature neutron diffraction structures of *N*-glycoprotein linkage models and analogs: structure refinement and trifurcated hydrogen bonds. J. Am. Chem. Soc. **133**, 10042–10045 (2011)
20. Mathiselvam, M., Loganathan, D., Varghese, B.: Synthesis of *N*-(β-D-glycuronopyranosyl)alkanamides and 1-(β-D-glycuronopyranosyl)-4-phenyl-[1–3]-triazoles as *N*-glycoprotein linkage region analogs:

examination of the effect of C5 substituent on the *N*-glycosidic torsion (ϕ_N) based on X-ray crystallography. Carbohydr. Res. **380**, 1–8 (2013)
21. Mathiselvam, M., Srivastava, A., Varghese, B., Pérez, S., Loganathan, D.: Synthesis and X-ray crystallographic investigation of *N*-(β-D-glycosyl)butanamides derived from GlcNAc and chitobiose as analogs of the conserved chitobiosylasparagine linkage of *N*-glycoproteins. Carbohydr. Res. **380**, 37–44 (2013)
22. Srivastava, A., Varghese, B,. Loganathan, D.: Synthesis and X-ray crystallographic investigation of N-(α-D-arabinopyranosyl)alkanamides as N-glycoprotein linkage region analogs. doi:10.1016/j.carres.2013.07.014.
23. Delbaere, L.T.J.: The molecular and crystal structures of 4-*N*-(2-acetamido-2-deoxy-β-D-glucopyranosyl)-L-asparagine trihydrate and 4-*N*-(β-D-glucopyranosyl)-L-asparagine monohydrate. The X-ray analysis of a carbohydrate-peptide linkage. Biochem. J. **143**, 197–205 (1974)
24. Ohanessian, J., Avenel, D., Neuman, A., Gillier-Pandraud, H.: Structure cristalline de la 2-acétamido-1-*N*-(L-aspart-4-oyl)-2-désoxy-β-D-glucopyranosylamine. Carbohydr. Res. **80**, 1–13 (1980)
25. Linkhosherstov, L.M., Novikova, O.S., Derevitskaja, V.A., Kochetkov, N.K.: A new simple synthesis of amino sugar β-D-glycosylamines. Carbohydr. Res. **146**, C1–C5 (1986)
26. Jeffrey, G.A.: Crystallographic studies of carbohydrates. Acta Crystallogr. **B46**, 89–103 (1990)
27. Koyama, Y., Shimanouchi, T., Iitaka, Y.: The crystal and molecular structures of *N*-methylchloroacetamide. Acta Crystallogr. **B27**, 940 (1971)
28. Peralta-Inga, Z., Johnson, G.P., Dowd, M.K., Rendleman, A.J., Stevens, E.D., French, A.D.: The crystal structure of the α-cellobiose · 2NaI · $2H_2O$ complex in the context of related structures and conformational analysis. Carbohydr. Res. **337**, 851–861 (2002)
29. French, A.D.: Combining computational chemistry and crystallography for a better understanding of the structure of cellulose. In: Horton, D. (ed.) Advances in Carbohydrate Chemistry and Biochemistry, vol. 67, pp. 19–93. Academic, Burlington (2012)
30. Marchessault, R.H., Perez, S.: Conformations of the hydroxymethyl group in crystalline aldohexopyranoses. Biopolymers **18**, 2369–2374 (1979)
31. Chu, S.S.C., Jeffrey, G.A.: The crystal structure of methyl β-maltopyranoside. Acta Crystallogr. **23**, 1038 (1967)
32. Bruker: APEX2, SAINT-Plus and XPREP. Bruker Axs Inc, Madison (2004)
33. Bruker: SADABS. Bruker AXS Inc, Wisconsin (1999)
34. Sheldrick, G.M.: SHELXL97, Program for Crystal Structure Refinement. Germany, University of Gottingen (1997)
35. Farrugia, L.J.: ORTEP-3 for windows-a version of ORTEP-III with a Graphical User Interface (GUI). J. Appl. Cryst. **30**, 565 (1997)
36. Bruno, I.J., Cole, J.C., Edgington, P.R., Kessler, M., Macrae, C.F., McCabe, P., Pearson, J., Taylor, R.: New software for searching the Cambridge structural database and visualizing crystal structure. Acta Crystallogr **B58**, 389–397 (2002)